Characterization of Portland cement concrete microstructure using the scanning acoustic microscope

Richard A. Livingston [a,*], Murli Manghnani [b], Manika Prasad [c]

[a]*Exploratory Research Team, Federal Highway Administration, HNR-2, 6300 Georgetown Pike, McLean, Virginia, 22101, USA*

[b]*Geophysics Department, University of Hawaii, Honolulu, Hawaii, USA*

[c]*Geophysics Laboratory, Stanford University, Stanford, California, USA*

Abstract

The scanning acoustic microscope has been applied to investigate several aspects of Portland cement concrete microstructure. This method uses ultrasound to image the local impedance at each point of a material. The impedance image highlights microstructural features that are difficult to observe with other imaging techniques. The topics investigated so far include the influence of aggregate composition on the development of the cement paste–aggregate interface, the nature of interfacial transition zone, and ettringite formation. Several types of gels have been observed, and these can be classified by their characteristic impedance values. Future work includes quantification of impedance values by first arrival times and the identification of Portland cement concrete phases by ultrasonic impedance spectroscopy. Published by Elsevier Science Ltd.

Keywords: Petrography; Scanning electron microscopy; Scanning acoustic microscopy; Microcracking; Portland cement

Portland cement concrete is a composite material made up of the hydrated cement matrix, fine (75 μm to 4.75 mm) aggregate, and coarse (>4.75 mm) aggregate. A major factor determining the strength of the material is the bond at the interface of the matrix and the aggregates [1]. However, it has been difficult to investigate these interfaces using conventional techniques [2].

The scanning acoustic microscope (SAM) provides a novel way to observe these interfaces. It uses acoustic waves to measure the mechanical properties of the constituents in the sample under investigation. The resulting image shows the impedance contrast among the constituents, which is determined by variations in their densities and elastic properties (velocity and attenuation). Thus, the SAM can provide images of the material that are complementary to optical and scanning electron microscope (SEM) images [3]. Furthermore, it can be used to make quantitative estimates of various parameters of the interfacial bond. This paper describes some preliminary results of a research program to apply the SAM to concrete interface problems.

1. Scanning acoustic microscopy

1.1. Operating principle

The acoustic microscope operates by launching ultrasound rays into the material specimen and detecting the reflected specular rays. The acoustic probe is illustrated in Fig. 1A. It consists of a piezoelectric transducer (ZnO film) located on top of a sapphire lens. The acoustic signals are generated in a pulsed mode to enable the transducer to function both as transmitter and receiver. The acoustic waves generated by the transducer are channeled through the sapphire lens and a coupling fluid, typically water, and brought to focus on the sample [4,5]. The waves reflected by the specimen return through the sapphire lens to the transducer, where they are detected.

As shown in Fig. 1B, the lens is scanned in a raster pattern over the specimen. The resulting map of the reflected ultrasound is converted into a digital electronic signal, which can be displayed on a conventional desktop computer monitor. Current versions of the instrument's software permit a gray- or color-scaled screen image with a resolution of 512 (256 for a low-frequency microscope) pixels in the x and y directions with 256 (8-bit) gray or color shades.

The reflection coefficient at the water–solid interface is determined by the elastic constants of the material. Varia-

* Corresponding author. Tel.: 703-285-2903; Fax: 703-285-2766; E-mail: dick.livingston@fhwa.dot.gov
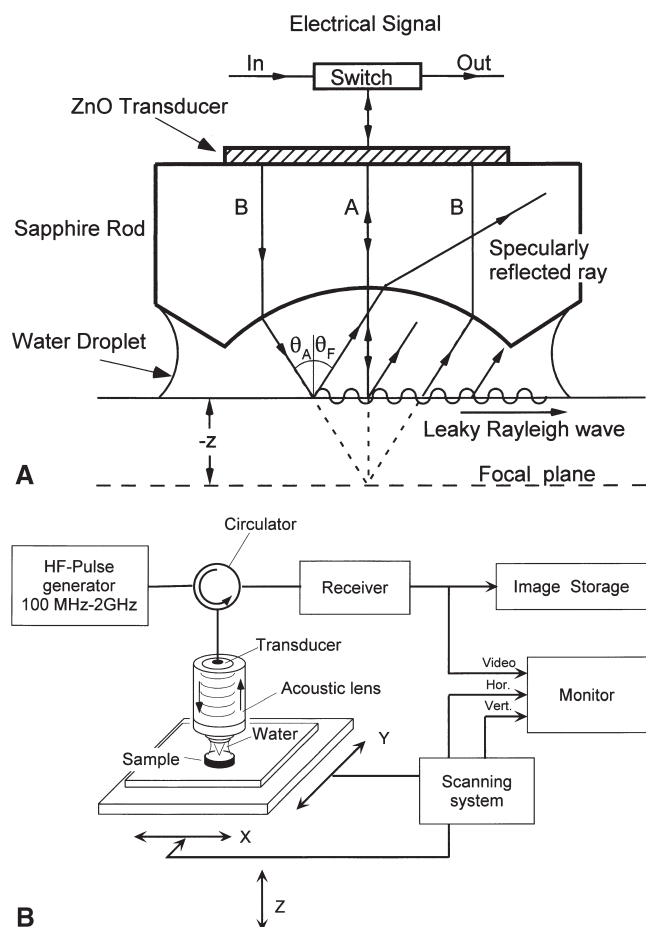
Fig. 1. (*A*) Ultrasonic wavepaths through the lens of the SAM. (*B*) Schematic diagram of the operation of the SAM.

tions in the elastic properties of the sample thus appear as variations in the gray or color values in an acoustic micrograph. The reflection coefficient is defined by Eq. (1):

$$R = \frac{Z_w - Z_s}{Z_w + Z_s} \tag{1}$$

where Z_w is the sound impedance of water and Z_s is that of the solid. A similar relationship exists for interfaces between solid phases at depth in the sample. In this case, Z_w and Z_s are replaced by Z_1 and Z_2, where the subscripts refer to the two solids. For water, $Z_w = 1.5 \times 10^6$ kg m^{-2}s^{-1}, and for solids it can range from 3 to 100×10^6 kg m^{-2}s^{-1}. For comparison, the impedance of air is approximately 4.29×10^3 kg m^{-2}s^{-1}.

2. Apparatus

Two different commercial models were used in this research. These were:

1. SAM50: A low-frequency acoustic microscope with a frequency range 25 to 100 MHz. The low-frequency microscope was operated at 50 MHz and used mainly to map larger areas and to estimate aggregate–cement-void distributions. Two types of scans made with SAM50 are discussed here: a C-scan, which is an x-y scan made at different depths (z-positions) in the sample, and a B-scan, which is an x-z scan. B-scans are produced by recording the reflections from the various layers or structures where an impedance contrast occurs. These scans are made through a time window with a fixed width and adjustable position. They can be compared to reflection seismic surveying on a microscale with seismograms constructed with a moving (scanning) source and receiver. A composite three-dimensional image is created by combining numerous B-scans made at various locations (y positions) on the sample.

2. ELSAM: A high-frequency acoustic microscope with a frequency range 0.4 to 2 GHz. In the high-frequency acoustic imaging of materials, such as rocks, the dominant role is played by Rayleigh waves that are excited at the surface of the specimen. These waves travel slower than longitudinal and shear waves, and they are confined to a subsurface depth of about one wavelength. By defocusing the specimen toward the lens relative to the focal plane, the impedance contrast can be made sensitive to interference between reflections associated with Rayleigh wave excitation and waves reflected normally from the specimen surface. The samples were analyzed at 0.4 and 1 GHz.

3. Sample preparation

The first set of samples to be investigated were originally mixed for another study [6]. These samples consisted of Portland cement mortar, and the fine aggregate consisted of either a granitic or a limestone sand, and some included silica fume. After curing, the samples were impregnated with epoxy resin.

For optimum results with the SAM, the specimens must have a very smooth surface. The allowable surface roughness decreases with increasing sound frequency. At 50 MHz, it is <30 mm and at 1 GHz it is <1.0 mm. The polishing of samples was carried out at the University of Hawaii using special instruments and a diamond grit. The samples were ground on each side and polished to a final finish of 0.1 mm. The two sides were parallel to about 1.0 mm. Due to variable stiffness of the cement matrix and aggregates, polishing required special care to prevent topographic effects between grains and matrix. A compromise was found at 400 MHz, which still gave good resolution and was not affected by topographic effects. Some specimens were split to make thin sections for optical and scanning electron microscopy.

4. Structure of voids

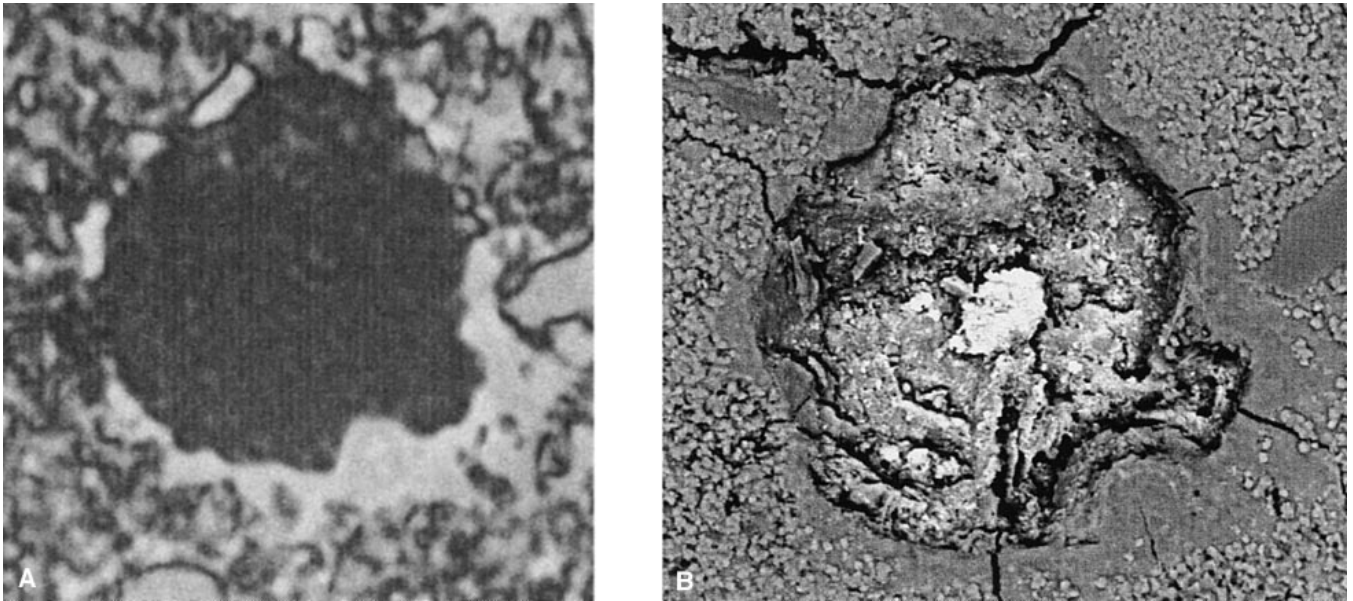Voids are typical features of Portland cement pastes. A 400-MHz SAM image of one is shown in Fig. 2A. Under

Fig. 2. (*A*) SAM image of void in mortar sample. Image size is 200 × 200 μm. (*B*) SEM image of the same void.

the SAM, a relatively broad rim can barely be seen (Fig. 2B). In the SAM image, a thin layer is revealed within the rim. In this image the contrast is produced almost entirely by normally reflected longitudinal waves; consequently, increasing brightness in Fig. 2A represents increasing impedance. Thus, the brightness of the layer around the void indicates a high im-

pedance and hence a relatively high hardness. Although this void was initially identified as an air bubble, it does not have the characteristic circular shape. Another possibility is that this feature is a Hadley shell [7]. Also apparent in Fig. 2B are several major cracks. These developed during the SEM examination of the sample, because of the vacuum conditions.

Fig. 3. SAM image of interfaces among cement matrix and aggregate grains. Image size is 1000 × 1000 μm.

5. Rayleigh fringe analysis

Fig. 3 is a SAM image of the cement mortar specimen made with granitic sand by Alexander et al. [6]. This shows a layer of cement matrix between two grains. Several features are apparent from the image. The shading difference between the grains shows that they have different elastic properties. This variation in elastic properties gives rise to a difference in the interference pattern between normally reflected longitudinal and Rayleigh waves. The grain on the right-hand side shows numerous interference fringes at grain and at subgrain boundaries. These interference fringes, produced by reflection of Rayleigh waves at discontinuities, have a characteristic spacing of 0.5 λ_R (λ_R = Rayleigh wavelength) The fringe pattern in this SAM image allows us to identify this grain as quartz. They have a spacing of 2.19 mm, giving a Rayleigh wave velocity, V_R ($V_R = \lambda_R f$, where f is frequency) of 3498 m/s, which is within the range of V_R for quartz (3410 m/s [4]). The gray-scale patterns within a grain implies an intragranular variation in elastic properties.

Finally, the dark line separating the cement matrix from the quartz grain indicates a lack of bond at this interface. The Rayleigh interference fringes parallel to the grain boundary prove the presence of a discontinuity between matrix and grain aggregate. The ability to detect this feature is unique to the SAM. It does not appear in the optical image and, as noted earlier, the SEM can introduce cracks in the sample. The development of bond between the feldspar grain and the matrix, and the lack of bond between the quartz grain and the matrix, indicates that the strength of the interface is influenced by the mineralogy of the aggregates.

6. Effect of grain mineralogy on interface development

The role of the aggregate grain composition on the interface is demonstrated in greater variety in Fig. 4. This is another image of same mortar sample discussed previously. In this image, there are several minerals present, including quartz, calcium-rich plagioclase, albite (sodium-rich feldspar), and hornblende (iron-rich amphibole). Around each of these minerals there is a different type of reaction rim. The albite grain boundary is severely eroded, indicating extensive reaction of the grain. There is some evidence of a transition zone for the plagioclase, but the development of a reaction rim is much less than for the albite. In contrast, there does not seem to be a reaction rim around the quartz. However, at the left end of this grain there is a gel phase. This may not be a result of a reaction with the quartz itself. Instead, it may have been produced by a reaction with the unidentified phase to the left. Finally, the hornblende grain is almost completely reacted. Again these features are very difficult to view with optical or scanning electron microscopy.

These results suggest that the simple classifications of aggregate type now used in the concrete industry, e.g., granitic, limestone, etc., may not be adequate to predict the ul-
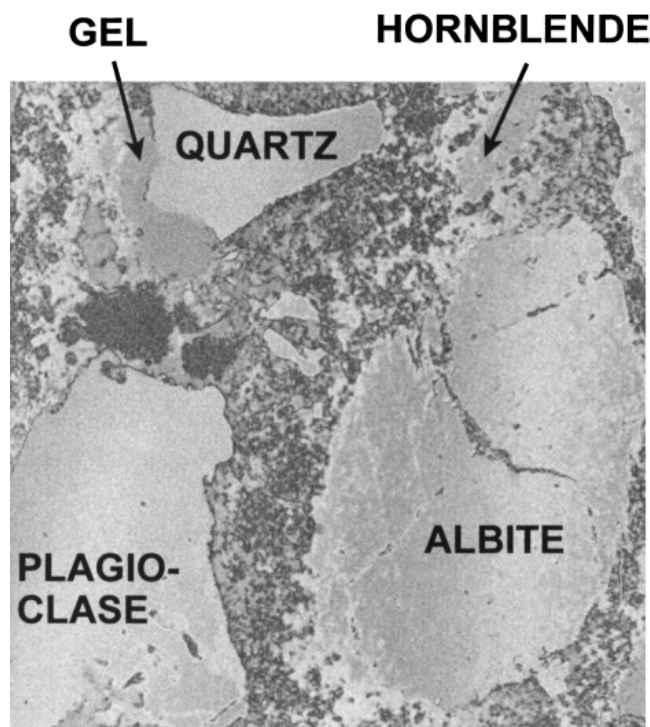

Fig. 4. SAM image of assorted granitic aggregate grains. Image size is 1000 × 1000 μm.

timate strength of the concrete. A more reliable classification system could require knowledge of the proportions of each type of mineral in the aggregate.

This SAM investigation of the influence of aggregate grain mineralogy also could be made quantitative through the application of automated image analysis. The size of the reaction rim around each grain could be computed. This parameter then could be investigated as a function of mineral composition, e.g., calcium/sodium ratio in feldspars. It also could be studied as a function of time of curing or of cement composition.

7. Future research

It has been demonstrated in this research that the SAM can be a useful tool for investigation of concrete. However, to become an effective standardized method, further research and development are required. This includes three major areas:

1. Development of internal impedance standards for calibration of the brightness of an image. These would be minerals of known impedance that would be added in trace quantities.
2. Determination of standard impedance values for the minerals found in concrete.
3. Application of automated image analysis software to SAM images.

Acknowledgments

References

[1] P.K. Mehta, P.J.M. Monteiro, Concrete: Structure, Properties and Materials, Prentice Hall, Englewood Cliffs, NJ, 1993.

[2] S. Mindess, M. Alexander, Mechanical phenomena at cement/aggregate interfaces, in: J. Skalny, S. Mindess (Eds.), Materials Science of Concrete IV, The American Ceramic Society, Westerville, OH, 1995, pp. 263–282.

[3] K.K. Aligizaki, B.R. Tittmann, G.A. Gordon, Comparison between optical microscopy and scanning acoustic microscopy for detecting flaws in concrete, Experimental Techniques 18 (1995) 24.

[4] G.A.D. Briggs, An Introduction to Scanning Acoustic Microscopy: Royal Microscopical Society Handbook, 12, Oxford University Press, Oxford, 1985.

[5] G.A.D. Briggs, Acoustic Microscopy: Monographs on the Physics and Chemistry of Materials, 47, Oxford Science Publications, Oxford, 1992.

[6] M.G. Alexander, S. Mindess, S. Diamond, L. Qu, Properties of paste-rock interfaces and their influence on composite behavior, Mat and Struct 28 (1995) 497–506.

[7] B.D. Barnes, S. Diamond, W. Dolch, Hollow shell hydration particles in bulk cement paste, Cem Conc Res 8 (2) (1978) 263–271.